

# A Valve-Enabled Sample Preparation Device with Isothermal Amplification for Multiplexed Virus Detection at the Point-of-Care

Carlos Manzanas, Md. Mahbubul Alam, Julia C. Loeb, John A. Lednicky, Chang-Yu Wu, and Z. Hugh Fan\*

Cite This: *ACS Sens.* 2021, 6, 4176–4184

Read Online

ACCESS |

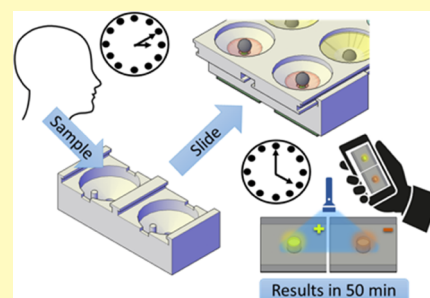
Metrics & More

Article Recommendations

Supporting Information

**ABSTRACT:** Early and accurate detection of severe acute respiratory syndrome coronavirus 2 (SARS-CoV-2) and influenza viruses at the point-of-care is crucial for reducing disease transmission during the current pandemic and future flu seasons. To prepare for potential cocirculation of these two viruses, we report a valve-enabled, paper-based sample preparation device integrated with isothermal amplification for their simultaneous detection. The device incorporates (1) virus lysis and RNA enrichment, enabled by ball-based valves for sequential delivery of reagents with no pipet requirement, (2) reverse transcription loop-mediated isothermal amplification, carried out in a coffee mug, and (3) colorimetric detection. We have used the device for simultaneously detecting inactivated SARS-CoV-2 and influenza A H1N1 viruses in 50 min, with limits of detection at 2 and 6 genome equivalents, respectively. The device was further demonstrated to detect both viruses in environmental samples.

**KEYWORDS:** SARS-CoV-2, COVID-19, influenza, valves, point-of-care, RT-LAMP, multiplexed detection



Severe acute respiratory syndrome coronavirus 2 (SARS-CoV-2) is the causative agent of the ongoing pandemic of coronavirus disease 2019 (COVID-19), which has resulted in over 4.3 million deaths worldwide as of August 10, 2021.<sup>1</sup> The main challenges associated with the COVID-19 pandemic include nonspecific clinical symptoms such as fever, a large number of asymptomatic individuals who are undiagnosed and contribute to the disease transmission, and lack of rapid diagnostic tools.<sup>2,3</sup> With expected cocirculation of respiratory viruses such as influenza viruses during flu seasons, these challenges require early and rapid virus detection at the point-of-care (POC) for reducing disease transmission. SARS-CoV-2 and influenza viruses can cause contagious respiratory illnesses with similar symptoms; thus, it is very important to have an ability to tell them apart by detecting these two viruses simultaneously for clinical and resource management.

The “gold-standard” test recommended by the World Health Organization (WHO) and the U.S. Centers for Disease Control and Prevention (CDC) for the detection of SARS-CoV-2 is the reverse transcription polymerase chain reaction (RT-PCR). This test is generally performed in a laboratory setting, takes several hours to complete, and requires expensive equipment and highly trained personnel. It often takes 1–2 days from sample collection to result-reporting because the collected sample needs to be transported to a laboratory, where it is often first stored frozen before being processed using nucleic acid extraction and purification protocols prior to RT-PCR. The sample preparation protocols also require laboratory equipment such as centrifuges and often include spin columns for a solid-

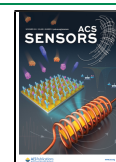
phase extraction step. Transportation and storage of samples are not needed if POC devices are used, reducing the sample-to-answer time. POC devices must include the sample preparation steps and require no laboratory equipment, thus facilitating their use by nonspecialized personnel. The existing POC systems such as Cepheid’s Xpert still require countertop equipment and are generally expensive. It should be noted that sample preparation steps have been eliminated from some SARS-CoV-2 detection systems.<sup>4,5</sup> However, these approaches can reduce detection sensitivity. For example, Thi et al. showed that the detection sensitivity was reduced from 97.5% with sample preparation to 86% without sample preparation in their reverse transcription loop-mediated isothermal amplification (RT-LAMP) assay systems.<sup>5</sup>

Some POC devices are based on antigen tests, such as the Panbio Covid-19 Ag Rapid Test device (Abbott),<sup>6</sup> and they are often used for rapid screening. However, the limited sensitivity of antigen tests can result in false negatives, leading to detrimental consequences during pandemics.<sup>7</sup> Efforts have been made to increase their detection sensitivity including various biosensors.<sup>8,9</sup> It is generally recognized that nucleic acid amplification tests (NAAT) are more sensitive, and they are

Received: August 12, 2021

Accepted: November 1, 2021

Published: November 12, 2021



often preferred over antigen tests, especially for reducing disease transmission by asymptomatic and presymptomatic persons.<sup>10</sup> Moreover, NAAT are easily adapted for the detection of different viruses<sup>11,12</sup> and can thus be configured to allow users to test for SARS-CoV-2, influenza, and other respiratory viruses at the same time. Multiplexed nucleic acid diagnostic tools will be useful to help control the COVID-19 pandemic and for influenza outbreaks, as well as for patient care.<sup>13</sup>

The first two SARS-CoV-2 NAAT POC kits approved for emergency use authorization (EUA) by the U.S. Food and Drug Administration (FDA) are the Lucira all-in-one test kit and the Cue test for home and over the counter (OTC) use.<sup>14</sup> The Lucira kit combines RT-LAMP with colorimetric detection, while the Cue test employs an unspecified isothermal amplification followed by electrochemical detection. Many POC testing platforms have been reported for influenza virus detection, including RT-LAMP devices,<sup>15–17</sup> microfluidics-based RT-PCR,<sup>18</sup> and other nucleic acid isothermal amplification assays.<sup>19</sup> Similarly, POC platforms for SARS-CoV-2 detection have been developed to incorporate RT-PCR,<sup>20</sup> RT-LAMP,<sup>5,21,22</sup> other amplification methods,<sup>23,24</sup> and those combined with CRISPR.<sup>25–27</sup>

However, little effort has been exerted for the development of POC platforms for simultaneous detection of SARS-CoV-2 and other respiratory viruses such as influenza viruses. Chung et al. used the BD MAX system,<sup>13</sup> and Mostafa et al. employed a Cepheid Xpert<sup>28</sup> for detection of SARS-CoV-2 and influenza viruses in healthcare settings. Others have developed portable platforms for detection of these viruses, but all of these require laboratory equipment for sample preparation.<sup>29,30</sup> Ji et al. reported a centrifugal RT-PCR microfluidic device for SARS-CoV-2 and influenza virus detection, but the device needs an instrument for spinning, thermocycling, and optical detection steps.<sup>30</sup> To our knowledge, there is no POC device available for simultaneous detection of SARS-CoV-2 and influenza viruses that includes all the necessary steps from sample to answer in a portable testing platform without the need of bulky or expensive laboratory equipment that requires power outlets at the time that this manuscript was written.

We have developed a duplex valve-enabled lysis, paper-based RNA enrichment, RNA amplification device (2-plex VLEAD) for multiplexed detection of SARS-CoV-2 and influenza viruses with no requirement for pipets and power outlets. This 2-plex VLEAD integrates (1) paper-based sample preparation using ball-based valves for sequential delivery of reagents and (2) RT-LAMP in a commercially available, battery-operated coffee mug with (3) colorimetric detection. The device consists of two sets of components fabricated in one platform with each set dedicated to one type of virus. The sample preparation process starts by sliding a part of the device to open valves sequentially that discharge various reagents for RNA extraction and purification while collecting RNA onto a paper pad. The reagents needed for sample preparation are preloaded in the device, thus requiring no pipetting at the POC. RNA collected on the paper pad is then amplified by RT-LAMP followed by colorimetric detection. This 2-plex VLEAD is low-cost and easy to use, providing results at the POC in a much shorter time than RT-PCR, with similar sensitivity.

## EXPERIMENTAL SECTION

**Device Fabrication.** The detection unit was made of a polycarbonate layer, a double-sided adhesive tape, two layers of thermoplastic films, and a paper pad as shown in Figure 1a and Figure

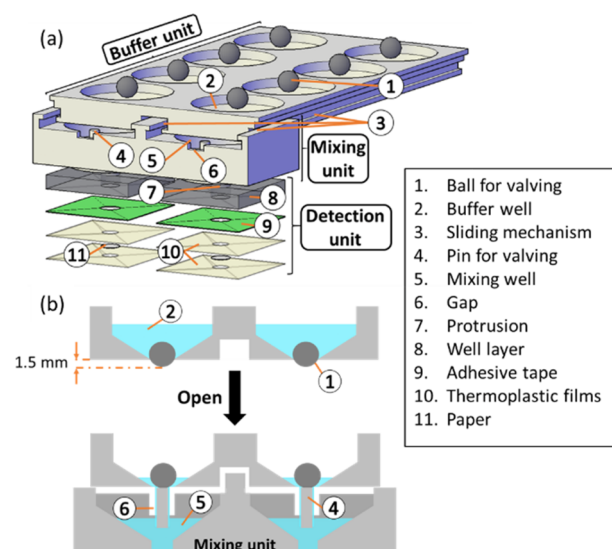


**Figure 1.** (a) Exploded view of the 2-plex VLEAD. The device consists of three components, including a buffer unit, a mixing unit, and two detection units. The buffer unit contains four wells in each side for storage of a lysis buffer, a binding buffer, and two washing buffers for sample preparation. In each well of the buffer unit, one stainless-steel ball is placed at the bottom that functions as the valve as explained in (b). The mixing unit has one well in each side, and it slides under the buffer unit through the sliding tracks on both sides and in the middle. At the bottom of each mixing well, a protrusion is created for inserting a detection unit. The detection unit contains a paper pad that is laminated between two thermoplastic films and attached to the polycarbonate well layer using a double-sided adhesive tape. The components are numerically marked and explained in the legend box. (b) Two-dimensional, cross-sectional view of the ball-based valve mechanism. The valves are closed when the balls function as plugs for the buffer wells while protruding slightly at the bottom. The valves are actuated by the pins in the mixing unit that lift the balls up when the pins are aligned with the balls after sliding, releasing the reagents into the mixing unit.

**S1b (Supporting Information).** The polycarbonate layer was shaped into a 2 cm × 2 cm square from a 3 mm-thick polycarbonate sheet (McMaster-Carr, Elmhurst, IL) using a CNC milling machine (Sherline Products, Vista, CA), and a well of 4 mm diameter was created in the center. To create the laminated paper pad, one piece of Whatman 1 chromatography paper (Fisher Scientific) and two 75 μm-thick polyester thermal bonding lamination films (Lamination Plus, Kaysville, UT, USA) were cut into 3.5 mm-diameter circles using a Graphtec Craft Robo-S cutting plotter (Graphtec Corporation, Yokohama, Japan). The paper was then sandwiched between the two films and passed through a heated laminator, GBC Catena 65 Roll Laminator (GBC, Lake Zurich, IL, USA), set at a rolling speed of “1” and at a temperature of 220 °F as previously described.<sup>31</sup> The laminated paper pad was attached to the polycarbonate container using double-sided adhesive tape (3M 9087 white bonding tape, R. S. Hughes, Sunnyvale, CA), forming the detection unit.

A commercial 3D printer, Ultimaker 3 (Ultimaker, Geldermalsen, Netherlands), was used to fabricate the buffer unit and the mixing unit. The devices were printed using polylactic acid (PLA) with polyvinyl alcohol (PVA) as a support material. The print layer height was set to 0.06 mm, and the infill density was set to 100% for PLA and PVA. The ball valves used for each well were 4.0 mm-diameter corrosion-resistant 316 stainless-steel balls (McMaster-Carr). To prevent accidental displacement or movement of the ball valves, a small amount of Akrowax 130 (Akrochem, Akron, OH, USA) was placed around the balls to melt and resolidify, forming a breakable bond between the balls and the buffer unit. An exploded view of the 2-plex VLEAD and the

valve concept are shown in Figure 1, and a picture of the device is shown in Figure S1.

**RT-LAMP Reaction.** Each 25  $\mu\text{L}$  RT-LAMP mix contained 2.5  $\mu\text{L}$  of a 10 $\times$  isothermal amplification buffer, 8 U of a Bst 2.0 WarmStart DNA polymerase, 7.5 U of a WarmStart RTx reverse transcriptase, 2.5  $\mu\text{L}$  of a 10 $\times$  concentrated primer mix, and final concentrations of 1.4 mM deoxynucleotide triphosphate (dNTPs) and 6 mM  $\text{MgSO}_4$ . The 25  $\mu\text{L}$  volume was filled using nuclease-free water (not DEPC-treated). Except for the nuclease-free water and dNTPs from Thermo Fisher (MA, USA), all other reagents in the RT-LAMP mix were obtained from New England Biolabs (NEB, Ipswich, MA, USA). The 10 $\times$  primer mix for SARS-CoV-2 contained 16  $\mu\text{M}$  FIP/BIP, 2  $\mu\text{M}$  F3/B3, and 8  $\mu\text{M}$  LF/LB (Table S1). The 10 $\times$  primer mix for influenza A H1N1 contained 16  $\mu\text{M}$  FIP/BIP, 2  $\mu\text{M}$  F3/B3, and 4  $\mu\text{M}$  LF/LB (Table S2). The primers were obtained from Integrated DNA Technologies (Coralville, Iowa, USA) and were chosen by following the literature.<sup>32,33</sup>

In addition, 0.5 units of the antarctic thermostable uracil-DNA glycosylase (UDG) and 0.7 mM deoxyuridine triphosphate (dUTP) were added to the 25  $\mu\text{L}$  RT-LAMP mix described above. UDG and dUTP were used to eliminate possible carryover contamination, reducing nonspecific amplification and potential false positives. UDG has been widely used to prevent carryover contamination without compromising sensitivity in LAMP and other nucleic acid amplification assays.<sup>34–36</sup> Initial work on the primer concentration comparison for SARS-CoV-2, the specificity tests, and the environmental sample experiments were carried out using the regular RT-LAMP mix. All other experiments were performed with UDG and dUTP added.

To achieve RT-LAMP without the need of connecting to a power outlet, we chose a commercially available, battery-powered coffee mug (Ember Technologies, Inc., Westlake Village, CA) as a heated water bath as we reported previously.<sup>31</sup> Prior to being placed in the coffee mug containing water at 62.5  $^\circ\text{C}$ , the detection units were sealed using two pieces of tape (Fellows) to cover the bottom and top parts. After 25 min of incubation, the detection units were taken out for colorimetric detection, which was carried out by adding 0.5  $\mu\text{L}$  of 10,000 $\times$  concentrate SYBR green I in dimethyl sulfoxide (Thermo Fisher). We used SYBR green for endpoint detection of amplicons because its color change can be visualized by the naked eyes or recorded using a smartphone camera. To help in visualization, an ULAKO blue LED flashlight (Amazon, WA, USA) powered by one AA battery was used to observe the green fluorescence if target viruses were present. The amplified products can also be verified by gel electrophoresis. Note that RT-LAMP produces a mixture of different sizes of amplicons, generating many gel bands as opposed to one specific gel band with RT-PCR.<sup>37</sup>

**Real-Time RT-LAMP.** We used a commercial real-time thermal cycler to verify the incubation time required for SARS-CoV-2 and influenza A H1N1 virus assays. The real-time RT-LAMP experiments were carried out by adding 0.5  $\mu\text{L}$  of a 10 $\times$  concentrate SYBR green I nucleic acid gel stain in dimethyl sulfoxide (Thermo Fisher) to the 25  $\mu\text{L}$  RT-LAMP reaction mix. The fluorescence signal from the reactions was read through the QuantStudio 3 real-time PCR system (Thermo Fisher).

For both viruses, four concentrations were used along with no-template controls (NTC), and three replications were carried out. For SARS-CoV-2 real-time assay, 10<sup>4</sup>, 10<sup>3</sup>, 10<sup>2</sup>, and 10 genome equivalents (GEs) were spiked into the 25  $\mu\text{L}$  RT-LAMP reactions. For influenza A H1N1 virus assay, RNAs of viruses in the amounts of 600, 60, 6, and 1.2 TCID<sub>50</sub> (median tissue culture infectious dose) were spiked into the 25  $\mu\text{L}$  RT-LAMP reactions.

For the experiments to study the effects of primer concentrations (Figure S2c), we used SARS-CoV-2 RNA of three RNA amounts (10<sup>4</sup>, 10<sup>3</sup>, and 10<sup>2</sup> GEs) and compared the effects of two different primer concentrations. The RT-LAMP mixtures were incubated for 45 min to analyze which primer conditions would give faster amplification without producing nonspecific amplification. For the endpoint colorimetric detection in Figure S2a, we compared RT-LAMP results after 20, 25, and 30 min of incubation at 62.5  $^\circ\text{C}$ . Three sets of repeat experiments were carried out for each primer concentration. The same

SARS-CoV-2 RNA concentration was used for all the positive controls (10<sup>2</sup> GEs).

**Assay Sensitivity and Specificity.** To assess the sensitivity of the RT-LAMP assay for detection of SARS-CoV-2, RNA was extracted from a stock of SARS-CoV-2/human/USA/UF-1/2020 (GenBank accession no. MT295464). The genome equivalents per microliter (GEs/ $\mu\text{L}$ ) of the extracted RNA were estimated from a standard curve based on an RT-PCR assay<sup>38</sup> and corresponded to approximately 1  $\times$  10<sup>6</sup> GEs/ $\mu\text{L}$ . Serial dilutions (10-fold) were made using RNA storage solution (Invitrogen), and 1  $\mu\text{L}$  of purified RNA of the different concentrations was used in the 25  $\mu\text{L}$  RT-LAMP reactions, along with an NTC.

For the influenza A H1N1 virus, RNA was extracted and purified using a Zymo Viral Magbead kit (Zymo Research) from a stock of the influenza virus H1N1 strain A/Mexico/4108/2009 that was at a titer of 6  $\times$  10<sup>6</sup> TCID<sub>50</sub>/mL. Again, 10-fold serial dilutions were made using RNA storage solution, and 1  $\mu\text{L}$  of purified RNA at different concentrations was added into the 25  $\mu\text{L}$  RT-LAMP reactions, along with an NTC. For more accurate results, different dilutions were made between 6 and 0.03 TCID<sub>50</sub>/ $\mu\text{L}$ .

We determined the detection specificities of SARS-CoV-2 and influenza A H1N1 virus assays by carrying out the following experiments: (a) we used the primer set for SARS-CoV-2 detection to test the genomic RNAs of SARS-CoV-2, influenza A H1N1, and CoV-OC43, respectively, to confirm if it would not produce nonspecific amplification for the latter two, and (b) we used the primer set for influenza A H1N1 virus detection to test these three virus RNAs. For both experiments, 1  $\mu\text{L}$  of each virus RNA sample was added into the 25  $\mu\text{L}$  RT-LAMP reactions, along with an NTC.

**Multiplexed Detection.** The 2-plex VLEAD operation starts with adding a 140  $\mu\text{L}$  sample into each mixing well, which is the recommended volume used in a commercial QIAamp Viral RNA mini kit (QIAGEN). Immediately after, the mixing unit slides to the first reservoirs of the buffer unit, which have been preloaded with 560  $\mu\text{L}$  of lysis buffer (AVL, QIAGEN), discharging them into the mixing unit to mix with each sample. To keep the 1:4:4 volume ratio of sample:lysis buffer:binding buffer as in the kit protocol, 560  $\mu\text{L}$  of ethanol has been preloaded into the second reservoirs as the binding buffer. After the lysis buffer flows down, the mixing unit is moved to the second reservoirs to discharge the binding buffer, which promotes RNA absorption onto the paper pad as the solution goes through the detection units. After these solutions go completely through the paper, the mixing unit is slid again one at a time to the third and fourth reservoirs, which are preloaded with 1 mL of AW1 and AW2 (QIAGEN) wash buffer, respectively. Finally, the detection units are removed from the mixing unit followed by adding the 25  $\mu\text{L}$  RT-LAMP mix into each unit and incubating them in the coffee mug at 62.5  $^\circ\text{C}$  for 25 min.

For heat-inactivated SARS-CoV-2 samples and in real-world situations, 140  $\mu\text{L}$  samples are added to the mixing wells as described above followed by the discharge of the lysis buffer through the ball valve. However, as a safety precaution for our experiments, the influenza A H1N1 virus samples were mixed with AVL at a ratio of 1:4 in a biosafety level 2+ laboratory prior to processing the sample in the device. Thus, in this case, the lysed sample would be added to the mixing unit followed by the discharge of the binding buffer, using only three of the four wells in the buffer unit.

**Environmental Samples.** Environmental samples were collected between February and March of 2020 by swabbing a handle of the main entry door of a building at the University of Florida, as described previously.<sup>39</sup> The environmental samples tested in this work were enumerated as samples #1, #2, #3, #4, and #5 corresponding to their collection on February 19, February 20, February 21, March 2, and March 4, respectively.<sup>39</sup> RNA was purified from the samples using a QIAamp Viral RNA mini kit, and the purified RNA was stored at  $-80$   $^\circ\text{C}$  in the presence of a SUPERase-In RNase inhibitor (Thermo Fisher). For our experiments, samples were created by mixing 3.5  $\mu\text{L}$  of purified RNA of the five different environmental samples with 14  $\mu\text{L}$  of AVL buffer and 14  $\mu\text{L}$  of ethanol in a biosafety hood. The 31.5  $\mu\text{L}$  mix was loaded into the detection unit using a pipette. After the sample mix had

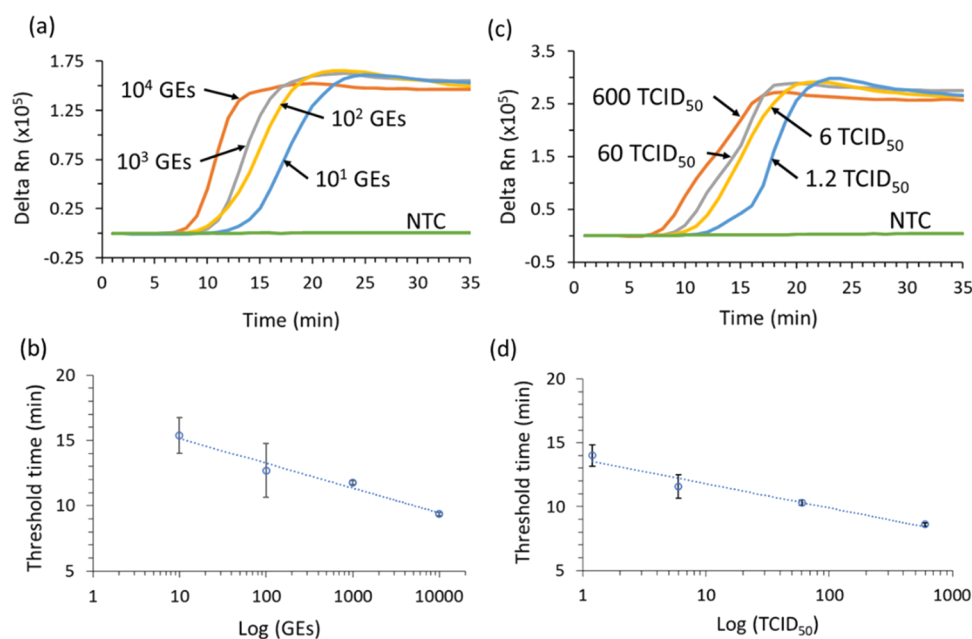


**Figure 2.** (a) Real-time RT-LAMP amplification for SARS-CoV-2 showing fluorescent signals of  $10^4$ ,  $10^3$ ,  $10^2$ , and 10 genome equivalents (GEs) as a function of the reaction time. NTC, no-template control. The average of three replicates was used. The y-axis represents the difference (Delta) between reactions (Rn) for the sample and the control. (b) Calibration curve between the threshold time (Ct) and SARS-CoV-2 GEs in each reaction (in the log scale). The error bars indicate one standard deviation, generated from three replicates of each concentration of SARS-CoV-2 RNA samples. (c) Real-time RT-LAMP amplification for the influenza A virus, showing fluorescent signals of 600, 60, 6, and 1.2 median tissue culture infectious dose (TCID<sub>50</sub>) of the influenza A virus as a function of the RT-LAMP time. NTC, no-template control. The average of three replicates was used. (d) Calibration curve between the threshold time (Ct) and influenza A virus TCID<sub>50</sub> in each reaction (in the log scale). The error bars indicate one standard deviation, generated from three replicates of each concentration of influenza A virus RNA samples.

completely gone through the paper pad, 100  $\mu$ L of AW1 was passed through the unit followed by 100  $\mu$ L of AW2. After RNA enrichment and purification, the detection units went through RT-LAMP amplification as described above.

Controls and samples were run in parallel for both viruses, SARS-CoV-2 and influenza A H1N1 viruses. Their preparation was in the following order: negative controls, samples, and positive controls. This order was chosen to reduce the opportunities of possible contamination during sample handling, preventing possible false positives. For the negative controls, nuclease-free water was added. For positive controls, 1  $\mu$ L of purified RNA of each virus was added to the respective RT-LAMP mix.

## RESULTS AND DISCUSSION

**Device Design and Fabrication.** Figure 1a shows the design of the 2-plex VLEAD for the simultaneous detection of SARS-CoV-2 and influenza A viruses, while a picture of the assembled device is shown in Figure S1 (Supporting Information). Additionally, the supplementary video shows the parts of the 2-plex VLEAD and the sample preparation process. The device consists of a buffer unit at the top, a mixing unit in the middle, and two detection units at the bottom. We borrowed the concept of our previously reported singleplex VLEAD device for Zika virus detection.<sup>31</sup> In addition to the difference in the multiplexing capability between singleplex and duplex devices, the 2-plex device has another sliding mechanism in the middle for an extra support. Since the 2-plex device simultaneously processes two samples in the same sequence, both detection units will be ready for the subsequent step. In addition to the multiplexing capability, the 2-plex VLEAD enables one user to operate at the POC, which is more advantageous than two singleplex VLEAD devices that are preferably operated by two people at the same time (or one

person with two devices operated in sequence). The 2-plex VLEAD also reduces fabrication cost and time compared to two singleplex devices.

The device integrates all the necessary steps for NAAT, including virus lysis, RNA enrichment and purification, amplification, and detection. Fluid-control valves are employed to perform sample preparation by sequential release of the reagents from the buffer unit into the mixing unit without the need of basic laboratory equipment. The valves consist of stainless-steel balls placed at the bottom of each buffer well to prevent the reagents from flowing down until desired. These ball-based valves protrude 1.5 mm from the bottom of the buffer unit so that the pins in the mixing unit, designed to be at the same level as the bottom surface of the buffer unit, lift the balls up allowing the reagents to flow down when the pins are aligned with the balls, as shown in Figure 1b. To prevent the balls from lifting up while sliding the mixing unit before the pins are aligned with the balls, two gaps are created as clearance at the top of each mixing well to let the balls pass. Additionally, to prevent ball displacement and fluid leakage during device transportation, a breakable bond is created between the ball and the reservoir using a biocompatible wax. First, a small piece of a wax is placed around each ball valve followed by heating the device to melt the wax. The wax is then cooled down to resolidify around the ball and create a bond to prevent any undesired ball movement. The bond is breakable later on when a pin lifts up the ball.

The RNA enrichment process is driven by the capillary forces generated by the chromatography paper in the detection units, eliminating the need of external equipment. An untreated cellulose chromatography paper was chosen for RNA enrichment because it has shown better results for RNA enrichment of influenza viruses when compared with the glass-fiber paper and

FTA card.<sup>17</sup> Additionally, the device does not require an elution step as in the QIAGEN kit, where the purified RNA needs to be eluted before amplification, which has significant disadvantages: (1) the purified RNA is diluted during elution and (2) not all the RNA on the column can be eluted. Involving no RNA transfer between tubes as in the lab operation, this device avoids possible contamination and degradation issues.

Compared to other multiplexed POC platforms developed for simultaneous detection of SARS-CoV-2 and influenza viruses, our platform offers a higher sensitivity and specificity than those antigen tests<sup>29</sup> due to amplification and genetic identification and processing of larger sample volumes (140  $\mu\text{L}$  in our device) than typical microfluidic platforms such as the centrifugal RT-PCR microfluidic devices that can process a few  $\mu\text{L}$  of samples.<sup>30</sup> The ability of processing a larger sample volume can lead to a lower limit of detection since more virus RNA is enriched onto the paper pad of the detection unit.

Compared to the Lucira kit mentioned above, our platform offers simultaneous detection of two pathogens rather than SARS-CoV-2 only. In addition, the Lucira kit uses nasal swab samples, while the 2-plex VLEAD can also process saliva samples,<sup>31</sup> which is more acceptable to users. Another difference is that we use a dye to interact with the amplicons directly, while the Lucira kit detects a pH change from amplification, in which the sensitivity can be affected by the buffer used.

To address the potential commercial use, we have calculated the cost of the 2-plex VLEAD and the related reagents. As shown in Table S3, each 2-plex device costs \$2.19 using a 3D printer. This price is expected to reduce significantly if injection molding is used for large-scale production. The total reagent cost for both SARS-CoV-2 and influenza virus assays is \$8.93 (Table S3). This is based on the retail price that we paid; the wholesale price is likely much lower. For comparison, each Lucira kit costs about \$50.

**RT-LAMP Reaction Time.** We determined the time needed for optimal RT-LAMP detection of the target virus using the QuantStudio-3 real-time amplification system. For SARS-CoV-2, all samples containing various concentrations of RNA reached a plateau within 25 min as shown in Figure 2a. The reactions were incubated for 35 min, and no nonspecific amplification was observed in the NTC. These results were reinforced by data in Figure S2, which confirmed that a 25 min RT-LAMP reaction time was sufficient to detect SARS-CoV-2 RNA in our device. This 25 min amplification time is significantly shorter than the conventional RT-PCR used for COVID-19 diagnosis.<sup>40,41</sup> Note that RT-LAMP involves many complicated reaction steps, and the resulting fluorescence signal does not necessarily correlate with the starting viral load. However, the threshold time ( $C_t$ ) measured by the instrument can be used to correlate with the viral load as in RT-PCR.<sup>42</sup> Figure 2b shows the calibration curve, indicating the feasibility of semiquantitative SARS-CoV-2 detection.

We used H1N1 pdm2009 as an example of the influenza A virus for this work, and the real-time RT-LAMP assay results are shown in Figure 2c. All samples in different concentrations reached a plateau within 20 min. The reactions were incubated for 35 min, and no nonspecific amplification was observed in the NTC. The results suggest that a 20 min incubation was sufficient for detecting influenza A viruses in our device. However, we used a 25 min incubation for simultaneous detection of SARS-CoV-2. Figure 2d shows the calibration curve between the threshold time and the influenza A virus amount, indicating that semiquantitative detection is feasible as shown previously.<sup>17</sup>

Note that the threshold time was automatically reported from the real-time PCR machine.

**Effects of Primer Concentrations.** For the detection of SARS-CoV-2 genomic RNA, we chose the RT-LAMP primers developed by Baek et al.<sup>32</sup> However, the primer concentrations used by Baek et al.<sup>32</sup> (5  $\mu\text{M}$  for external primers F3 and B3, 20  $\mu\text{M}$  for internal primers FIP and BIP, and 5  $\mu\text{M}$  for loop primers LF and LB) are different from what we previously reported (2  $\mu\text{M}$  for F3/B3, 16  $\mu\text{M}$  for FIP/BIP, and 8  $\mu\text{M}$  for LF/LB),<sup>31</sup> which were based on recommendations by the RT-LAMP reagent manufacturer, NEB. Therefore, we compared these two procedures, and the results using either real-time RT-LAMP or colorimetric detection are shown in Figure S2.

Using the NEB primer concentrations reported previously,<sup>31</sup> a color change in the reaction tube was observed after 20 min of RT-LAMP for a sample containing 100 GEs of virus RNA (Figure S2b). The color change was more pronounced after 25 min of RT-LAMP in another tube (note that separate tubes must be used for each condition because the colorimetric detection was carried out at the end of RT-LAMP). In contrast, no color change was observed after 20 min of RT-LAMP, and the color change was observed only after 25 min of RT-LAMP when we employed the primer concentrations used by Baek et al.<sup>32</sup> These results were confirmed using real-time RT-LAMP assay (Figure S2c), in which the signals were observed a bit later under the conditions used by Baek et al. than under the NEB conditions for all three concentrations of SARS-CoV-2 viruses. This difference in the RT-LAMP time between two experimental conditions was larger for  $10^2$  GEs of virus RNA than  $10^3$  and  $10^4$  GEs of virus RNA. It should be noted that good specificity was attained using both approaches, with no nonspecific amplification after 45 min of RT-LAMP when no template was present (NTC in Figure S2c). On the other hand, the condition used by Baek et al. showed better linear correlation between the number of GEs and the threshold time than the NEB conditions (Figure S2d). For the following experiments, we chose to employ the NEB conditions.

**Assay Sensitivity and Specificity.** The RT-LAMP assay for SARS-CoV-2 detection showed high sensitivity and a limit of detection (LoD) of 2 GEs. We first studied the assay using 100, 10, and 1 GEs of SARS-CoV-2 as shown in Figure 3a,b and observed the positive signals in all three replicates of 100 and 10 GEs. For 1 GE samples, we observed only two out of three replicates, indicating that the LoD of our assay is at least 10 GEs. The results were confirmed using gel electrophoresis (Figure 3c). Note that these RNA samples were directly combined with the RT-LAMP mix for testing in the detection units. To further determine the LoD between 1 and 10 GEs, we carried out the second experiment using 10, 5, 2, and 1 GEs of SARS-CoV-2 and observed positive signals in all three replicates of 10, 5, and 2 GEs as shown in Figure S3. Similarly, we observed positive signals in only two out of three replicates for 1 GE samples. These results are summarized in Table 1. The capability of detecting 2 GEs of SARS-CoV-2 shows that our device has a comparable limit of detection to, if not better than, the gold-standard RT-PCR assay developed by CDC (which is 5 copies/reaction<sup>40,43</sup>), as well as other RT-LAMP assays for SARS-CoV-2 detection in the literature.<sup>21,44</sup> Note that the 2-GE LoD was obtained from samples containing RNA that is equivalent to the corresponding virus genome.

Similarly, the assay for the influenza A virus showed an LoD of 0.06 TCID<sub>50</sub>, which is approximately 6 GEs (based on about 100 GEs per virion and 1 virion corresponds to 1 TCID<sub>50</sub> unit). We

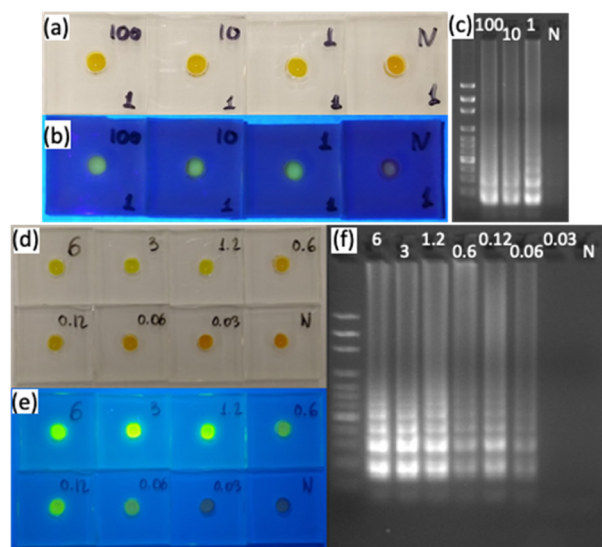


**Figure 3.** (a) Pictures of the detection units taken under room light after RT-LAMP assay at 62.5 °C for 25 min. Amounts of SARS-CoV-2 RNA are marked on the devices, 100, 10, and 1 GE, as well as a negative control (N). (b) Same devices as (a) under a blue LED. (c) Gel electrophoresis of those samples in (a). The left lane is for the DNA ladder, while other lanes are marked at the top. (d) Pictures of the detection units taken under room light after RT-LAMP assay at 62.5 °C for 25 min. Amounts of influenza A virus RNA are indicated, 6, 3, 1.2, 0.6, 0.12, 0.06, and 0.03 TCID<sub>50</sub>, as well as a negative control (N). (e) Same devices as (d) under a blue LED. (f) Gel electrophoresis of those samples in (d). The left lane is for the DNA ladder, while other lanes are marked at the top.

**Table 1. RT-LAMP Assay Results for SARS-CoV-2 Detection**

RNA amount (GEs)	first experiment <sup>a</sup>	second experiment <sup>a</sup>	total <sup>a</sup>
100	3/3		3/3
10	3/3	3/3	6/6
5		3/3	3/3
2		3/3	3/3
1	2/3	2/3	4/6
NTC	0/3	0/3	0/6

<sup>a</sup>Note: the results are listed as the number of positive results/the number of experiments.

studied the RT-LAMP assay using concentrations from 6 TCID<sub>50</sub> to 0.003 TCID<sub>50</sub> of influenza A viruses and observed the positive signals in all five replicates of 0.06 TCID<sub>50</sub> and higher, as shown in Figure 3d,e. However, for samples containing less than 0.06 TCID<sub>50</sub>, we did not observe signals in any replicates. The results were also confirmed by gel electrophoresis (Figure 3f). This LoD of 6 GEs is at least similar, if not better, when compared to other RT-LAMP assays for detection of influenza viruses at the POC, which is in the range of 10 to 100 copies per reaction.<sup>15,16</sup> Overall, RT-LAMP assays for both SARS-CoV-2 and influenza A viruses have an LoD of <10 GEs per reaction, which is comparable to the gold-standard RT-PCR assays.

Figure 4 shows that both assays for SARS-CoV-2 and influenza A viruses have good specificity in our devices. The SARS-CoV-2 assay showed no cross-reactivity with influenza virus A and human coronavirus OC43 (CoV-OC43) as shown in Figure 4a,b. CoV-OC43 is a coronavirus that is known to infect humans and cause the common colds. Similarly, the influenza A virus assay showed no cross-reactivity with SARS-CoV-2 and CoV-OC43 as shown in Figure 4c,d. These experimental results

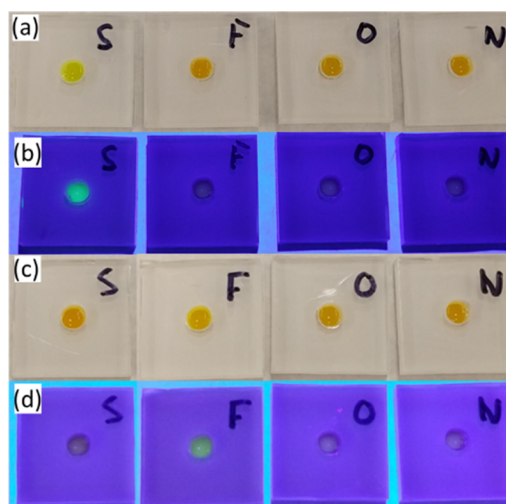


**Figure 4.** (a) Pictures of the detection units under room light using SARS-CoV-2 assay with samples containing SARS-CoV-2 RNA (S), influenza A virus RNA (F), CoV-OC43 RNA (O), and no RNA (N). (b) Same devices in (a) under a blue LED. (c) Pictures of the detection units under room light using influenza A virus assay with samples containing influenza A virus RNA (F), SARS-CoV-2 RNA (S), CoV-OC43 RNA (O), and no RNA (N). (d) Pictures of the same devices in (c) under a blue LED.

are expected because the SARS-CoV-2 primers had been previously tested against a panel of RNA samples of related coronaviruses, a panel of human and avian influenza viruses, and a panel of other respiratory disease-causing viruses.<sup>32</sup> The RT-LAMP primers for influenza A H1N1 viruses had also been tested previously against other subtypes of influenza A viruses, though they have not been tested against any coronaviruses.<sup>33</sup>

**Device Testing Using Control Samples.** Using the device in Figure 1a, we were able to detect SARS-CoV-2 and influenza A viruses using inactivated virus samples (Figure 5a). We obtained heat-inactivated SARS-CoV-2 samples, containing the cell lysate and the supernatant from Vero E6 cells infected with SARS-CoV-2, from BEI Resources (USA-WA1/2020, NR-52286), which were deposited by CDC. The influenza A H1N1 pdm2009 was produced by the laboratory of Dr. John Lednicky as reported previously,<sup>45</sup> and the samples in cell culture media were lysed with AVL buffer in a biosafety level 2+ environment to meet the safety requirement. The total time for sample preparation to flow the respective solutions through the device and to enrich RNA onto the paper pad in the detection unit was about 25 min.

**Multiplexed Detection Using Environmental Samples.** We tested five environmental samples that were spared from another study.<sup>39</sup> These samples were identified with numbers only and blinded to the researchers who performed 2-plex assays. The results were then provided back to the investigator of the previous study and compared with those results using RT-PCR.<sup>39</sup> The comparison shows that we were able to detect both viruses, SARS-CoV-2 and influenza A H1N1 in sample #3, which is in agreement with the results obtained by RT-PCR and sequencing.<sup>39</sup> Figure 5b shows the detection results of sample #2 that contains the influenza A virus only. All results for five environmental samples are summarized in Table 2. Since the samples were the leftovers from the previous study,<sup>39</sup> some of them are insufficient for replicate experiments. Overall, however, we demonstrated the decent specificity and sensitivity of our assay, with only 1 false positive and 1 false negative among a total

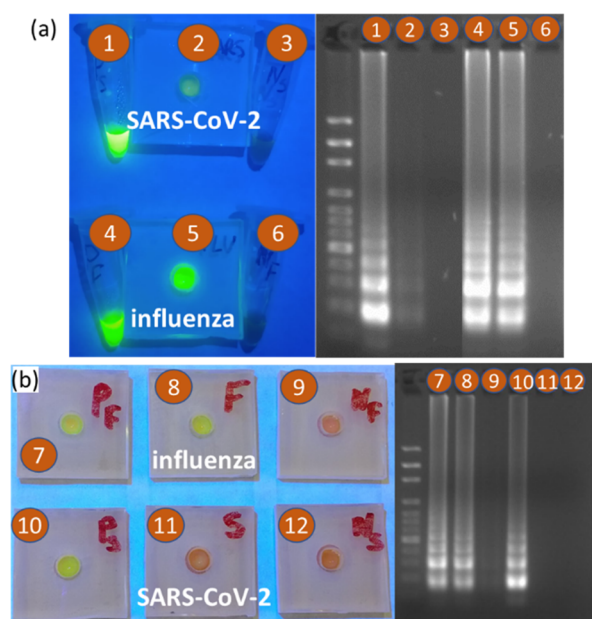


**Figure 5.** (a) Simultaneous detection of heat-inactivated SARS-CoV-2 and influenza A H1N1 viruses using the 2-plex VLEAD device. Pictures of (1) a positive control in a tube for SARS-CoV-2 assay, (2) a detection unit after processing the SARS-CoV-2 sample, (3) a negative control in a tube for SARS-CoV-2 assay, (4) a positive control in a tube for influenza A virus assay, (5) a detection unit after processing the influenza A H1N1 virus sample, and (6) a negative control in a tube for influenza A virus assay, are on the left. Pictures were taken under a blue LED. Gel electrophoresis results of these samples are shown on the right, in which the left lane is the DNA ladder, while other lanes are marked at the top. (b) Multiplexed detection of SARS-CoV-2 and influenza A H1N1 viruses in environmental sample #2. Pictures of detection units for influenza A H1N1 virus assay: (7) a positive control, (8) sample #2, and (9) a negative control and for SARS-CoV-2 assay: (10) a positive control, (11) sample #2, and (12) a negative control, are on the left. Gel electrophoresis results of these samples are shown on the right, in which the left lane is the DNA ladder, while other lanes are marked at the top.

**Table 2.** RT-LAMP Assay for Environmental Samples and Its Comparison with RT-PCR

sample no.	SARS-CoV-2 detected <sup>a</sup>	RT-PCR <sup>b</sup>	influenza A H1N1 detected <sup>a</sup>	RT-PCR <sup>b</sup>
1	0/1	no	1/1	yes
2	0/2	no	2/2	yes
3	2/2	yes	2/2	yes
4	0/2	no	2/3	yes
5	0/2	no	1/2	no

<sup>a</sup>Note: the results are listed as the number of positive results/the number of experiments. <sup>b</sup>“Yes” or “no” indicates whether the SARS-CoV-2 or influenza A H1N1 virus was present or absent in the corresponding samples based on RT-PCR.

of 19 experiments. The results correspond to a 90.0% (9/10) positive percent agreement (PPA), an 88.9% (8/9) negative percent agreement (NPA), and an overall percent agreement of 89.5% (17/19).

## CONCLUSIONS

We have developed a rapid and sensitive multiplexed POC testing platform, the 2-plex VLEAD, for simultaneous detection of SARS-CoV-2 and influenza A H1N1 viruses in 50 min (~25

min for sample preparation and ~25 min for RT-LAMP assay). To our knowledge, our 2-plex VLEAD is the first POC platform that can simultaneously detect both viruses using NAAT integrating all the necessary steps including sample preparation, RNA amplification, and detection into a single platform without the need of bulky or sophisticated laboratory equipment. Other platforms have been reported for POC detection using NAAT for SARS-CoV-2<sup>21,46</sup> or influenza viruses,<sup>15,18,47</sup> for laboratory settings using NAAT for both viruses,<sup>48,49</sup> and for healthcare setting detection approved by the FDA for emergency use authorization.<sup>50</sup> Nevertheless, they are not for multiplexed detection of SARS-CoV-2 and other respiratory viruses such as influenza viruses at the POC. A multiplexed POC platform will be useful for testing individuals suspected of either SARS-CoV-2 or influenza infections, especially during flu seasons.

The 2-plex VLEAD can be adapted for testing different variants of SARS-CoV-2, subtypes of influenza viruses (e.g., A and B), or other types of viruses, depending on the need and potential outbreaks. The reagents can be prepackaged in the buffer unit for storage and transportation for testing at the POC, and the ball-based valves have been shown no leakage for several weeks when wax was used to fix the ball to the respective buffer well. The RT-LAMP mix can also be preloaded in disposable pipettes and stored in ice coolers. One alternative is to use lyophilized RT-LAMP reagents as reported elsewhere.<sup>51,52</sup> Therefore, the platform has the potential to help reduce disease transmission by bringing the tests close to patients or other sites in need.

One limitation of the colorimetric detection used in this work is its binary results: yes or no, representing the presence or absence of viruses. It is sufficient for some situations, for example, when people only need to know if they are infected or not. However, it is unsatisfactory for other circumstances, for instance, when people want to know their viral loads. For the latter, an instrument capable of real-time detection is required.

## ASSOCIATED CONTENT

### Supporting Information

The Supporting Information is available free of charge at <https://pubs.acs.org/doi/10.1021/acssensors.1c01718>.

(Table S1) Primer sequences for the SARS-CoV-2 assay, (Table S2) primer sequences for the influenza A H1N1 assay, (Table S3) platform cost analysis, (Figure S1) device picture, (Figure S2) primer concentration optimization, (Figure S3) experimental results related to the limit of detection, and (Figure S4) picture of detection units in the coffee mug (PDF)

Video explaining the device components and steps from sample preparation to colorimetric detection (MOV)

## AUTHOR INFORMATION

### Corresponding Author

Z. Hugh Fan – *Interdisciplinary Microsystems Group, Department of Mechanical and Aerospace Engineering, University of Florida, Gainesville, Florida 32611, United States; J. Crayton Pruitt Family Department of Biomedical Engineering, University of Florida, Gainesville, Florida 32611, United States; [orcid.org/0000-0002-1812-8016](https://orcid.org/0000-0002-1812-8016); Email: [hfan@ufl.edu](mailto:hfan@ufl.edu)*

## Authors

**Carlos Manzanás** – Interdisciplinary Microsystems Group, Department of Mechanical and Aerospace Engineering, University of Florida, Gainesville, Florida 32611, United States; [orcid.org/0000-0002-3460-0077](https://orcid.org/0000-0002-3460-0077)

**Md. Mahbulul Alam** – Department of Environmental and Global Health, University of Florida, Gainesville, Florida 32610, United States; Emerging Pathogens Institute, University of Florida, Gainesville, Florida 32610, United States

**Julia C. Loeb** – Department of Environmental and Global Health, University of Florida, Gainesville, Florida 32610, United States; Emerging Pathogens Institute, University of Florida, Gainesville, Florida 32610, United States

**John A. Lednicky** – Department of Environmental and Global Health, University of Florida, Gainesville, Florida 32610, United States; Emerging Pathogens Institute, University of Florida, Gainesville, Florida 32610, United States

**Chang-Yu Wu** – Department of Environmental Engineering Sciences, University of Florida, Gainesville, Florida 32611, United States; [orcid.org/0000-0002-2100-8816](https://orcid.org/0000-0002-2100-8816)

Complete contact information is available at:

<https://pubs.acs.org/10.1021/acssensors.1c01718>

## Author Contributions

C.M. performed the research, developed the methods, curated the data, and drafted the paper. M.M.A. and J.C.L. prepared virus samples and purified the virus RNA. J.A.L. acquired funding, provided the samples, developed the methods, provided resources, and supervised the work. C.-Y.W. acquired funding and supervised the work. Z.H.F. developed the concept, acquired funding, developed the methods, provided resources, supervised the work, and drafted the paper. All authors have reviewed and approved the final manuscript for publication.

## Notes

The authors declare no competing financial interest.

## ACKNOWLEDGMENTS

This work was supported in part by the US National Science Foundation (CBET-2030844), the US National Institutes of Health (R01AI158868 and R01AI155735), and the University of Florida, USA.

## REFERENCES

- (1) WHO WHO Coronavirus (COVID-19) Dashboard, <https://covid19.who.int/>, accessed on August 10, 2021.
- (2) Phua, J.; Weng, L.; Ling, L.; Egi, M.; Lim, C. M.; Divatia, J. V.; Shrestha, B. R.; Arabi, Y. M.; Ng, J.; Gomersall, C. D.; Nishimura, M.; Koh, Y.; Du, B. Intensive care management of coronavirus disease 2019 (COVID-19): challenges and recommendations. *Lancet Respir. Med.* **2020**, *8*, 506–517.
- (3) Johansson, M. A.; Quandelacy, T. M.; Kada, S.; Prasad, P. V.; Steele, M.; Brooks, J. T.; Slayton, R. B.; Biggerstaff, M.; Butler, J. C. SARS-CoV-2 Transmission From People Without COVID-19 Symptoms. *JAMA Netw. Open* **2021**, *4*, No. e2035057.
- (4) Zhang, C.; Zheng, T.; Wang, H.; Chen, W.; Huang, X.; Liang, J.; Qiu, L.; Han, D.; Tan, W. Rapid One-Pot Detection of SARS-CoV-2 Based on a Lateral Flow Assay in Clinical Samples. *Anal. Chem.* **2021**, *93*, 3325–3330.
- (5) Thi, V. L. D.; Herbst, K.; Boerner, K.; Meurer, M.; Kremer, L. P.; Kirrmaier, D.; Freistaedter, A.; Papagiannidis, D.; Galmozzi, C.; Stanifer, M. L.; Boulant, S.; Klein, S.; Chlanda, P.; Khalid, D.; Barreto Miranda, I.; Schnitzler, P.; Kräusslich, H. G.; Knop, M.; Anders, S. A

colorimetric RT-LAMP assay and LAMP-sequencing for detecting SARS-CoV-2 RNA in clinical samples. *Sci. Transl. Med.* **2020**, *12*, 556.

(6) Berger, A.; Nsoga, M. T. N.; Perez-Rodriguez, F. J.; Aad, Y. A.; Sattonnet-Roche, P.; Gayet-Ageron, A.; Jaksic, C.; Torriani, G.; Boehm, E.; Kronig, I.; et al. Diagnostic accuracy of two commercial SARS-CoV-2 antigen-detecting rapid tests at the point of care in community-based testing centers. *PLoS One* **2021**, *16*, No. e0248921.

(7) Scohy, A.; Anantharajah, A.; Bodéus, M.; Kabamba-Mukadi, B.; Verroken, A.; Rodriguez-Villalobos, H. Low performance of rapid antigen detection test as frontline testing for COVID-19 diagnosis. *J. Clin. Virol.* **2020**, *129*, 104455.

(8) Zhong, J.; Rösch, E. L.; Viereck, T.; Schilling, M.; Ludwig, F. Toward Rapid and Sensitive Detection of SARS-CoV-2 with Functionalized Magnetic Nanoparticles. *ACS Sens.* **2021**, *6*, 976–984.

(9) Ventura, B. D.; Cennamo, M.; Minopoli, A.; Campanile, R.; Censi, S. B.; Terracciano, D.; Portella, G.; Velotta, R. Colorimetric Test for Fast Detection of SARS-CoV-2 in Nasal and Throat Swabs. *ACS Sens.* **2020**, *5*, 3043–3048.

(10) La Marca, A.; Capuzzo, M.; Paglia, T.; Roli, L.; Trenti, T.; Nelson, S. M. Testing for SARS-CoV-2 (COVID-19): a systematic review and clinical guide to molecular and serological in-vitro diagnostic assays. *Reprod. Biomed. Online* **2020**, *41*, 483–499.

(11) Yarbrough, M. L.; Burnham, C.-A. D.; Anderson, N. W.; Banerjee, R.; Ginocchio, C. C.; Hanson, K. E.; Uyeki, T. M. Influence of Molecular Testing on Influenza Diagnosis. *Clin. Chem.* **2018**, *64*, 1560–1566.

(12) Vos, L. M.; Bruning, A. H. L.; Reitsma, J. B.; Schuurman, R.; Riezebos-Brilman, A.; Hoepelman, A. I. M.; Oosterheert, J. J. Rapid Molecular Tests for Influenza, Respiratory Syncytial Virus, and Other Respiratory Viruses: A Systematic Review of Diagnostic Accuracy and Clinical Impact Studies. *Clin. Infect. Dis.* **2019**, *69*, 1243–1253.

(13) Chung, H. Y.; Jian, M. J.; Chang, C. K.; Lin, J. C.; Yeh, K. M.; Chen, C. W.; Chiu, S. K.; Wang, Y. H.; Liao, S. J.; Li, S. Y.; Hsieh, S. S. Novel dual multiplex real-time RT-PCR assays for the rapid detection of SARS-CoV-2, influenza A/B, and respiratory syncytial virus using the BD MAX open system. *Emerging Microbes Infect.* **2021**, *10*, 161–166.

(14) CDC In Vitro Diagnostics EUAs - Molecular Diagnostic Tests for SARS-CoV-2 Food and Drug Administration 2020.

(15) Jung, J. H.; Park, B. H.; Oh, S. J.; Choi, G.; Seo, T. S. Integration of reverse transcriptase loop-mediated isothermal amplification with an immunochromatographic strip on a centrifugal microdevice for influenza A virus identification. *Lab Chip* **2015**, *15*, 718–725.

(16) Ma, Y.-D.; Chen, Y.-S.; Lee, G.-B. An integrated self-driven microfluidic device for rapid detection of the influenza A (H1N1) virus by reverse transcription loop-mediated isothermal amplification. *Sens. Actuators, B* **2019**, *296*, 126647.

(17) Jiang, X.; Loeb, J. C.; Pan, M.; Tilly, T. B.; Eiguren-Fernandez, A.; Lednicky, J. A.; Wu, C.-Y.; Fan, Z. H. Integration of Sample Preparation with RNA-Amplification in a Hand-Held Device for Airborne Virus Detection. *Anal. Chim. Acta* **2021**, 338542.

(18) Ferguson, B. S.; Buchsbaum, S. F.; Wu, T. T.; Hsieh, K.; Xiao, Y.; Sun, R.; Soh, H. T. Genetic analysis of H1N1 influenza virus from throat swab samples in a microfluidic system for point-of-care diagnostics. *J. Am. Chem. Soc.* **2011**, *133*, 9129–9135.

(19) Wu, L. T.; Thomas, L.; Curran, M. D.; Ellis, J. S.; Parmar, S.; Goel, N.; Sharma, P. I.; Allain, J. P.; Lee, H. H. Duplex molecular assay intended for point-of-care diagnosis of influenza A/B virus infection. *J. Clin. Microbiol.* **2013**, *51*, 3031–3038.

(20) Gibani, M. M.; Toumazou, C.; Sohbaty, M.; Sahoo, R.; Karvela, M.; Hon, T. K.; De Mateo, S.; Burdett, A.; Leung, K. Y. F.; Barnett, J. Assessing a novel, lab-free, point-of-care test for SARS-CoV-2 (CovidNudge): a diagnostic accuracy study. *Lancet Microb.* **2020**, *1*, e300–e307.

(21) Ganguli, A.; Mostafa, A.; Berger, J.; Aydin, M. Y.; Sun, F.; Ramirez, S. A. S.; Valera, E.; Cunningham, B. T.; King, W. P.; Bashir, R. Rapid isothermal amplification and portable detection system for SARS-CoV-2. *Proc. Natl. Acad. Sci. U. S. A.* **2020**, *117*, 22727–22735.

(22) Zhu, X.; Wang, X.; Han, L.; Chen, T.; Wang, L.; Li, H.; Li, S.; He, L.; Fu, X.; Chen, S.; Xing, M.; Chen, H.; Wang, Y. Multiplex reverse

transcription loop-mediated isothermal amplification combined with nanoparticle-based lateral flow biosensor for the diagnosis of COVID-19. *Biosens. Bioelectron.* **2020**, *166*, 112437.

(23) Assennato, S. M.; Ritchie, A. V.; Nadala, C.; Goel, N.; Tie, C.; Nadala, L. M.; Zhang, H.; Datir, R.; Gupta, R. K.; Curran, M. D.; Lee, H. H. Performance Evaluation of the SAMBA II SARS-CoV-2 Test for Point-of-Care Detection of SARS-CoV-2. *J. Clin. Microbiol.* **2020**, *59*, e01262–e01220.

(24) El Wahed, A. A.; Patel, P.; Maier, M.; Pietsch, C.; Ruster, D.; Bohlken-Fascher, S.; Kissenkotter, J.; Behrmann, O.; Frimpong, M.; Diagne, M. M. Suitcase Lab for Rapid Detection of SARS-CoV-2 Based on Recombinase Polymerase Amplification Assay. *Anal. Chem.* **2021**, *93*, 2627–2634.

(25) Ding, X.; Yin, K.; Li, Z.; Lalla, R. V.; Ballesteros, E.; Sfeir, M. M.; Liu, C. Ultrasensitive and visual detection of SARS-CoV-2 using all-in-one dual CRISPR-Cas12a assay. *Nat. Commun.* **2020**, *11*, 4711.

(26) Ramachandran, A.; Huyke, D. A.; Sharma, E.; Sahoo, M. K.; Huang, C.; Banaei, N.; Pinsky, B. A.; Santiago, J. G. Electric field-driven microfluidics for rapid CRISPR-based diagnostics and its application to detection of SARS-CoV-2. *Proc. Natl. Acad. Sci. U. S. A.* **2020**, *117*, 29518–29525.

(27) Moon, J.; Kwon, H. J.; Yong, D.; Lee, I. C.; Kim, H.; Kang, H.; Lim, E. K.; Lee, K. S.; Jung, J.; Park, H. G.; Kang, T. Colorimetric Detection of SARS-CoV-2 and Drug-Resistant pH1N1 Using CRISPR/dCas9. *ACS Sens* **2020**, *5*, 4017–4026.

(28) Mostafa, H. H.; Carroll, K. C.; Hicken, R.; Berry, G. J.; Manji, R.; Smith, E.; Rakeman, J. L.; Fowler, R. C.; Leelawong, M.; Butler-Wu, S. M. Multicenter Evaluation of the Cepheid Xpert Xpress SARS-CoV-2/Flu/RSV Test. *J. Clin. Microbiol.* **2021**, *59*, e02955–20.

(29) Stambaugh, A.; Parks, J. W.; Stott, M. A.; Meena, G. G.; Hawkins, A. R.; Schmidt, H. Optofluidic multiplex detection of single SARS-CoV-2 and influenza A antigens using a novel bright fluorescent probe assay. *Proc. Natl. Acad. Sci. U. S. A.* **2021**, *118*, No. e2103480118.

(30) Ji, M.; Xia, Y.; Loo, J. F.-C.; Li, L.; Ho, H.-P.; He, J.; Gu, D. Automated multiplex nucleic acid tests for rapid detection of SARS-CoV-2, influenza A and B infection with direct reverse-transcription quantitative PCR (dirRT-qPCR) assay in a centrifugal microfluidic platform. *RSC Adv.* **2020**, *10*, 34088.

(31) Jiang, X.; Loeb, J. C.; Manzanos, C.; Lednický, J. A.; Fan, Z. H. Valve-Enabled Sample Preparation and RNA Amplification in a Coffee Mug for Zika Virus Detection. *Angewandte Chemie International Edition* **2018**, *57*, 17211–17214.

(32) Baek, Y. H.; Um, J.; Antigua, K. J. C.; Park, J. H.; Kim, Y.; Oh, S.; Kim, Y. I.; Choi, W. S.; Kim, S. G.; Jeong, J. H.; Chin, B. S.; Nicolas, H. D. G.; Ahn, J. Y.; Shin, K. S.; Choi, Y. K.; Park, J. S.; Song, M. S. Development of a reverse transcription-loop-mediated isothermal amplification as a rapid early-detection method for novel SARS-CoV-2. *Emerg Microbes Infect* **2020**, *9*, 998.

(33) Nakauchi, M.; Yoshikawa, T.; Nakai, H.; Sugata, K.; Yoshikawa, A.; Asano, Y.; Ihira, M.; Tashiro, M.; Kageyama, T. Evaluation of reverse transcription loop-mediated isothermal amplification assays for rapid diagnosis of pandemic influenza A/H1N1 2009 virus. *J. Med. Virol* **2011**, *83*, 10.

(34) Longo, M. C.; Berninger, M. S.; Hartley, J. L. Use of uracil DNA glycosylase to control carry-over contamination in polymerase chain reactions. *Gene* **1990**, *93*, 125–128.

(35) Hsieh, K.; Mage, P. L.; Csordas, A. T.; Eisenstein, M.; Soh, H. T. Simultaneous elimination of carryover contamination and detection of DNA with uracil-DNA-glycosylase-supplemented loop-mediated isothermal amplification (UDG-LAMP). *Chem. Commun.* **2014**, *50*, 3747–3749.

(36) Lamb, L. E.; Bartolone, S. N.; Ward, E.; Chancellor, M. B. Rapid detection of novel coronavirus/Severe Acute Respiratory Syndrome Coronavirus 2 (SARS-CoV-2) by reverse transcription-loop-mediated isothermal amplification. *PLoS One* **2020**, *15*, No. e0234682.

(37) Notomi, T.; Okayama, H.; Masubuchi, H.; Yonekawa, T.; Watanabe, K.; Amino, N.; Hase, T. Loop-mediated isothermal amplification of DNA. *Nucleic Acids Res.* **2000**, *28*, E63.

(38) Lednický, J. A.; Lauzardo, M.; Fan, Z. H.; Jutla, A.; Tilly, T. B.; Gangwar, M.; Usmani, M.; Shankar, S. N.; Mohamed, K.; Eiguren-Fernandez, A.; Stephenson, C. J.; Alam, M. M.; Elbadry, M. A.; Loeb, J. C.; Subramaniam, K.; Waltzek, T. B.; Cherabuddi, K.; Morris, J. G., Jr; Wu, C. Y. Viable SARS-CoV-2 in the air of a hospital room with COVID-19 patients. *Int J Infect Dis* **2020**, *100*, 476.

(39) Lednický, J.; Salemi, M.; Subramaniam, K.; Waltzek, T. B.; Sabo-Attwood, T.; Loeb, J. C.; Hentschel, S.; Tagliamonte, M. S.; Marini, S.; Alam, M. M.; et al. Earliest detection to date of SARS-CoV-2 in Florida: Identification together with influenza virus on the main entry door of a university building, February 2020. *PLoS One* **2021**, *16*, No. e0245352.

(40) CDC (2020) CDC 2019–Novel Coronavirus (2019-nCoV) Real-Time RT-PCR Diagnostic Panel.

(41) Bustin, S. A.; Nolan, T. RT-qPCR Testing of SARS-CoV-2: A Primer. *Int. J. Mol. Sci.* **2020**, *21*, 3004.

(42) Nguyen, D. V.; Nguyen, V. H.; Seo, T. S. Quantification of Colorimetric Loop-mediated Isothermal Amplification Process. *Bio-Chip J.* **2019**, *13*, 158–164.

(43) Lu, X.; Wang, L.; Sakthivel, S. K.; Whitaker, B.; Murray, J.; Kamili, S.; Lynch, B.; Malapati, L.; Burke, S. A.; Harcourt, J.; Tamin, A.; Thornburg, N. J.; Villanueva, J. M.; Lindstrom, S. US CDC Real-Time Reverse Transcription PCR Panel for Detection of Severe Acute Respiratory Syndrome Coronavirus 2. *Emerg Infect Dis* **2020**, *26*, 1654.

(44) Rodriguez-Manzano, J.; Malpartida-Cardenas, K.; Moser, N.; Pennisi, I.; Cavuto, M.; Miglietta, L.; Moniri, A.; Penn, R.; Satta, G.; Randell, P.; et al. Handheld Point-of-Care System for Rapid Detection of SARS-CoV-2 Extracted RNA in under 20 min. *ACS Cent. Sci.* **2021**, *7*, 307–317.

(45) Sanpui, P.; Zheng, X.; Loeb, J. C.; Bisesi, J. H.; Khan, I. A.; Afrooz, A. R.; Liu, K.; Badireddy, A. R.; Wiesner, M. R.; Ferguson, P. L.; et al. Single-walled carbon nanotubes increase pandemic influenza A H1N1 virus infectivity of lung epithelial cells. *Part Fibre Toxicol* **2014**, *11*, 66.

(46) Österdahl, M. F.; Lee, K. A.; Lochlainn, M. N.; Wilson, S.; Douthwaite, S.; Horsfall, R.; Sheedy, A.; Goldenberg, S. D.; Stanley, C. J.; Spector, T. D.; Steves, C. J. Detecting SARS-CoV-2 at point of care: preliminary data comparing loop-mediated isothermal amplification (LAMP) to polymerase chain reaction (PCR). *BMC Infect Dis* **2020**, *20*, 783.

(47) Abe, T.; Segawa, Y.; Watanabe, H.; Yotoryama, T.; Kai, S.; Yasuda, A.; Shimizu, N.; Tojo, N. Point-of-care testing system enabling 30 min detection of influenza genes. *Lab Chip* **2011**, *11*, 1166–1167.

(48) Zhang, Y.; Tanner, N. A. Development of multiplexed reverse-transcription loop-mediated isothermal amplification for detection of SARS-CoV-2 and influenza viral RNA. *BioTechniques* **2021**, *70*, 167–174.

(49) Nörz, D.; Hoffmann, A.; Aepfelbacher, M.; Pfefferle, S.; Lütgehetmann, M. Clinical evaluation of a fully automated, laboratory-developed multiplex RT-PCR assay integrating dual-target SARS-CoV-2 and influenza A/B detection on a high-throughput platform. *J. Med. Microbiol.* **2021**, *70*, DOI: 10.1099/jmm.0.001295.

(50) Hansen, G.; Marino, J.; Wang, Z. X.; Beavis, K. G.; Rodrigo, J.; Labog, K.; Westblade, L. F.; Jin, R.; Love, N.; Ding, K.; Garg, S.; Huang, A.; Sickler, J.; Tran, N. K. Clinical Performance of the Point-of-Care cobas Liat for Detection of SARS-CoV-2 in 20 Minutes: a Multicenter Study. *J. Clin. Microbiol.* **2021**, *59*, e02811–20.

(51) Toppings, N. B.; Mohon, A. N.; Lee, Y.; Kumar, H.; Lee, D.; Kapoor, R.; Singh, G.; Oberding, L.; Abdullah, O.; Kim, K.; Berenger, B. M.; Pillai, D. R. A rapid near-patient detection system for SARS-CoV-2 using saliva. *Sci. Rep.* **2021**, *11*, 13378.

(52) Juscamayta-López, E.; Valdivia, F.; Horna, H.; Tarazona, D.; Linares, L.; Rojas, N.; Huaringa, M. A Multiplex and Colorimetric Reverse Transcription Loop-Mediated Isothermal Amplification Assay for Sensitive and Rapid Detection of Novel SARS-CoV-2. *Front Cell Infect Microbiol* **2021**, *11*, 653616.